ELSEVIER

Surface Science 365 (1996) 394–402

surface science

Adsorption and reaction of magnesium on $Cr_2O_3(0001)/Cr(110)$

M. Bender, I.N. Yakovkin [1], H.-J. Freund *

Lehrstuhl für Physikalische Chemie I, Ruhr-Universität Bochum, D-44780 Bochum, Germany

Received 7 February 1996; accepted for publication 15 April 1996

Abstract

We report on the adsorption and reaction of magnesium on $Cr_2O_3(0001)/Cr(110)$ thin films. X-ray photoelectron spectroscopy (XPS) and X-ray induced Auger-spectroscopy (XAES) reveal the formation of magnesium oxide and chromium metal. The validity of bulk thermodynamic calculations for the estimation of chemical reactivity on surfaces is critically revisited.

Keywords: Alkaline earth metals; Auger electron spectroscopy; Cr_2O_3; Low energy electron diffraction (LEED); Surface chemical reaction; X-ray photoelectron spectroscopy

1. Introduction

Thin oxide films have been investigated as model systems for bulk oxide surfaces in the past in order to be able to apply electron spectroscopies while circumventing sample charging and problems with sample cooling [1]. These systems can now be used to study problems of interest in catalysis. A special topic in this field is the modification of an oxide surface by doping the sample with alkali and alkaline earth species (AAES) [2]. On elemental surfaces, adsorption of AAES has been studied in detail [3] and is well understood in relation to the interplay between geometric and electronic structure [4]. Surface chemistry in these cases involves surface reconstruction [5] and alloy formation [6] induced by the charge transfer from AAES towards the metal surfaces which is generally observed.

In contrast, adsorption of AAES on oxide surfaces has only been rarely studied in the past, and a thorough understanding of the interplay between geometric and electronic structure has been reported only in the case of TiO_2 [7]. Two new types of reactions occur in the surface chemistry of oxides due to the presence of oxygen. These two additional types of reaction are oxygen transfer from the oxide substrate into the AAES adlayer, and the formation of mixed oxides.

In our previous work we have shown that the system Na/NiO(111)/Ni(111) undergoes a reaction of complete oxygen transfer, finally leading to metallic nickel and sodium oxide on the surface of the nickel oxide layer [8]. Additionally we observed the reaction of sodium oxide with excess nickel oxide forming a mixed oxide species i.e. a sodium nickelate.

In the present work we find clear evidence for chromium metal and concomitant MgO formation in the system $Mg/Cr_2O_3(0001)/Cr(110)$. This is in contrast to the situation found for

* Corresponding author. Fax: +49 234 7094182; e-mail: hajo@marvin3.pc.ruhr-uni-bochum.de

[1] Permanent address: Institute of Physics, Ukrainian Academy of Science, Prospekt Nauki 46, Kiev 252028, Ukraine.

PII S0039-6028(96)00742-X

$Na/Cr_2O_3(0001)/Cr(110)$ where reduction to metallic chromium is not observed [9]. The present paper studies the chemistry of magnesium on chromium oxide $Cr_2O_3(0001)/Cr(110)$ thin films by the use of X-ray induced photoelectron spectroscopy and Auger spectroscopy (photon-induced) as experimental methods. The validity of thermodynamics for an estimation of oxygen transfer reactivities in the present case is critically discussed.

2. Experimental

The experiments were performed in a UHV chamber with a background pressure of 2×10^{-10} Torr. The chamber was equipped with a VSW XPS/XAES system, a conventional Omikron LEED system as well as a Leybold–Heraeus sputter gun. Sample preparation has been extensively described in previous papers [10]. Magnesium was thermally deposited from a pressed pellet consisting of a mixture of MgO, Al and CaO, which was confined in a Knudsen cell. After outgassing the source, the pressure never exceeded 4×10^{-10} Torr during the deposition procedure. For deposition the source was run at stabilized currents of about 2 A. After a warm-up time of approximately 5 min a shutter provided a rapid exposure of the sample at a constant deposition rate.

The calibration of the magnesium source output was carried out in a deposition series on the pure Cr(110) metal crystal surface at constant geometry and stabilized source current of 2.2 A. The sample temperature was kept constant at 90 K during the deposition. After each deposition the sample was warmed up to 300 K in order to anneal the adsorbate.

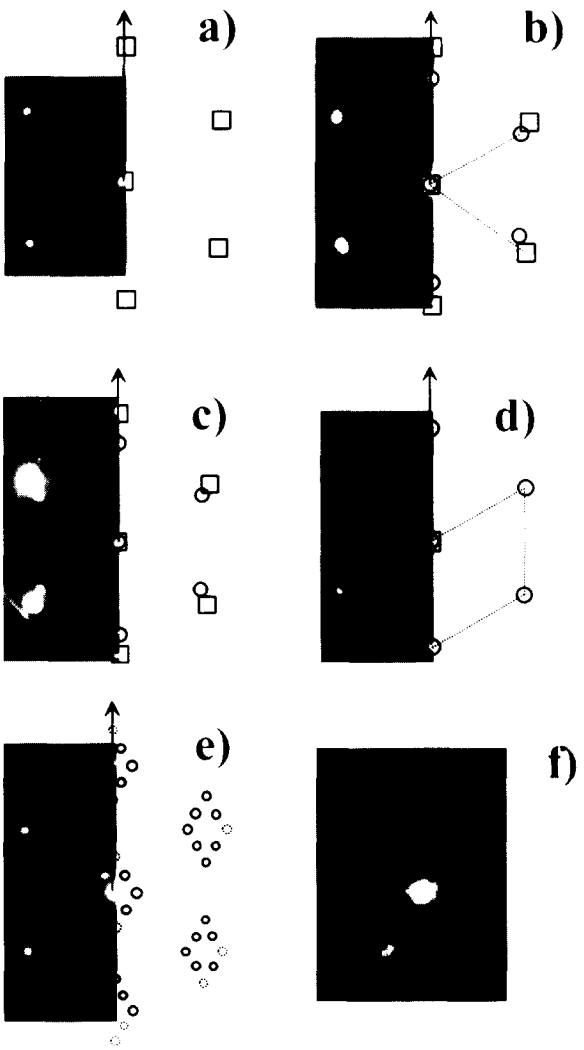

Fig. 1. LEED patterns for the Mg/Cr(110) system: (a) Clean Cr(110) surface; (b) ≈0.5 ML Mg/Cr(110); (c) ≈1.4 ML Mg/Cr(110); (d) ≈8 ML Mg/Cr(110); (e) ≈1.5 ML Mg/Cr(110) after heating a Mg multilayer coverage to 540 K; (f) details of the superstructure in (e), assigned to multiple scattering processes.

3. Results and discussion

The surface structure was checked by LEED at various Mg coverages [11]. The clean Cr(110) substrate surface shows a rectangular spot arrangement (Fig. 1a). With increasing magnesium coverage, deposited at room temperature, these spots are accompanied by a hexagon of less intense spots closer to the (0,0) spot (Fig. 1b) indicating the formation of a Mg(0001) lattice via layer-by-layer growth similar to literature data [12]. Very weak spots are observed around the substrate spots due to multiple scattering. The multiple scattering spots as well as the Cr(110) substrate spots vary upon further magnesium deposition (Fig. 1c) and are attenuated when multilayer coverages are reached (Fig. 1d). The size of the Mg(0001) hexagonal unit

mesh vector is determined relative to the substrate lattice vectors to be 3.2 Å which is identical to that of the (0001) basal plane vector in bulk magnesium [13].

With two Mg atoms in a (0001) unit mesh of 26.6 $Å^2$ area, the atom density in a monolayer is calculated to be 7.5×10^{14} cm^{-2} yielding a deposition rate of $4 \pm 0.5 \times 10^{12}$ cm^{-2} s^{-1}. The relative amount of Mg was measured via the Mg 1s XPS intensity. The Mg 1s intensity depends linearly on the deposition time as shown in Fig. 2. The change in slope at 190 ± 25 s deposition time is ascribed to the completion of the first magnesium monolayer [14].

The Mg 1s XPS intensity of this atom density is estimated from Fig. 2 to be 1.8 ± 0.2 arb. units. Thus the coverage can be estimated from either the deposition time or the Mg 1s XPS intensity.

Upon deposition of magnesium on the chromium oxide Cr_2O_3(0001)/Cr(110) surface at 90 K sample temperature, the quality of the LEED pattern becomes blurred as the coverage is increased. At multilayer coverage no sign of long range order is found and additional spots indicating superstructures have not been observed.

The Cr $2p_{3/2}$ XPS signals for increasing Mg coverage are shown in Fig. 3. The coverage was

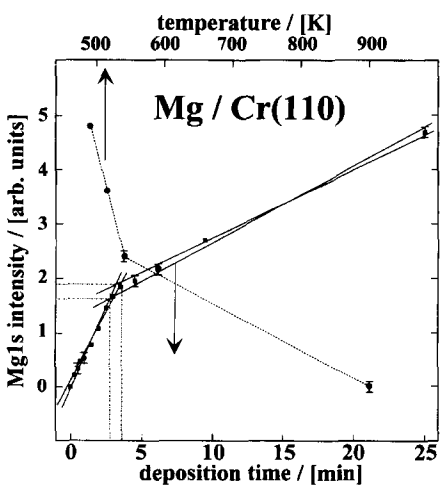

Fig. 2. Normalized intensity of the XPS Mg 1s signal in the system Mg/Cr(110) as a function of deposition time (squares) and as a function of temperature starting with a thick multilayer coverage (circles).

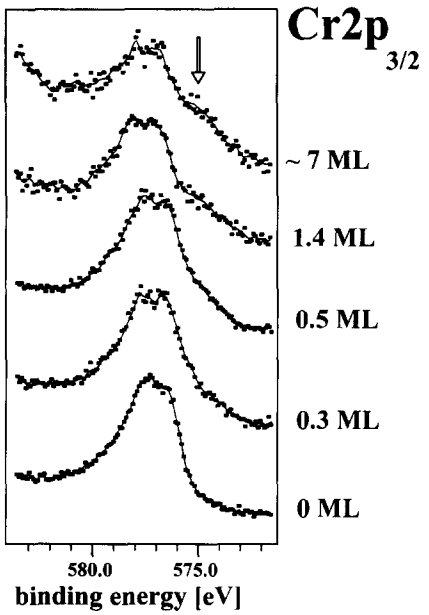

Fig. 3. Cr $2p_{3/2}$ XPS spectra of a deposition series of magnesium on chromium oxide at 90 K substrate temperature. The coverage has been determined by comparing the Mg 1s intensity with the data in Fig. 1. The arrow indicates intensity filling in at the lower binding energy side. The spectra were taken at 65° off-normal detection angle.

estimated corresponding to an evaluation of the Mg 1s intensity (Fig. 2). With increasing coverage a little intensity (arrow) is filling in at the low binding energy side. The main signal shifts to higher binding energies compared to the clean oxide surface. We ascribe this shift to band bending which is prominent in adsorption experiments on non-metal substrates [3,8]. Fig. 4 documents the difference between the spectra of the clean and the Mg-covered oxide surface at multilayer coverage i.e. at about 7 ML. In contrast to Fig. 3, the spectra (Fig. 4a and b) were taken with a pass energy of 22 eV instead of 10 eV in order to achieve a sufficient signal-to-noise ratio. Before performing the difference spectrum calculation, the spectrum of the Mg covered surface was shifted appropriately, i.e. by 0.3 eV to lower binding energy, accounting for the above mentioned band-bending effect. The difference spectrum (Fig. 4c) is compared to the spectrum of the clean Cr(110) metal surface (Fig. 4d) in the right panel. It indicates the presence of chromium metal on the surface in the

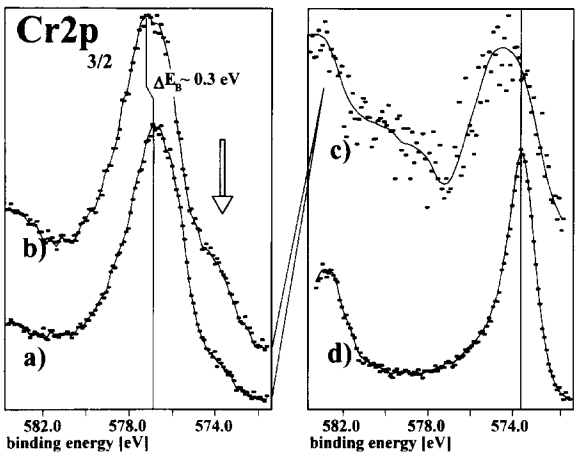

Fig. 4. Cr $2p_{3/2}$ XPS difference spectrum (c) between the spectrum of the clean (a) and the multilayer covered chromium oxide surface (b) in comparison to the spectrum (d) of the chromium metal Cr(110) surface.

case of a multilayer Mg coverage. Additionally, the main signal of the difference spectrum exhibits a tailing to higher binding energies. We ascribe this to the fact that the metal phase is not uniform, i.e. it may contain small particles of different sizes which are well known to show higher core-level binding energies as compared to the bulk metal [15].

The chemical state of magnesium on the oxide surface was investigated by XPS and XAES spectra which are shown in Fig. 5a and b respectively. For small coverages in the submonolayer regime, the Mg 1s signal is located at 1304.8 eV and is ascribed to magnesium oxide. At multilayer coverages it shifts to 1303.0 eV, which corresponds to the value of magnesium metal [16]. Due to a FWHM of about 2 eV a further distinction of different magnesium species is not possible on the basis of the XPS data alone, but can be achieved by considering the corresponding Auger $KL_{23}L_{23}$ spectra. Chemical shifts in the Auger energy of magnesium are dominated by final state effects as has been discussed for sodium adsorbates [8]. In metallic magnesium the double core-hole in the final state is screened by the polarizable metal electrons, whereas in magnesium oxide this screening is provided mainly by the less polarizable oxygen valence-band electrons. Hence, in the former case

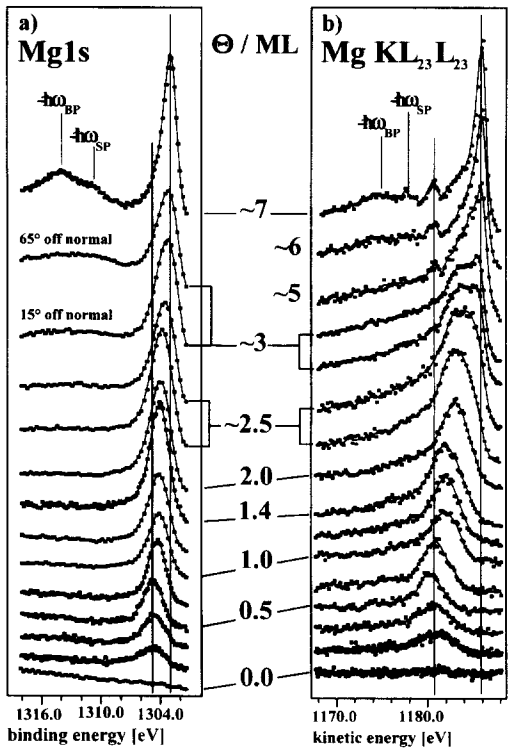

Fig. 5. Mg 1s XPS (left panel) and $KL_{23}L_{23}$-Auger (right panel) spectra as a function of magnesium coverage. If not indicated otherwise, the spectra were taken with 15° off-normal detection angle. The plasmon loss features are discussed in detail in the text.

the kinetic energy of the Auger electrons is higher by about 5 eV. At low coverages the Mg $KL_{23}L_{23}$ signal is found at 1180.6 eV kinetic energy (Fig. 5b) in line with literature data for magnesium oxide [16]. This line steadily shifts to higher kinetic energy with increasing exposure, finally reaching the value of 1186 eV for bulk Mg at large coverages. Note that these shifts are larger than those expected from band bending etc. in photoemission.

To interpret the shifts we assume that magnesium aggregates of increasing size form upon increasing coverage. The polarizability of the valence electrons of the aggregates will change simultaneously. Consequently, the observed Mg Auger line shifts towards higher kinetic energy with increasing coverage.

It is worth noting that even above 2 ML the

spectrum still differs from that of magnesium metal. We ascribe this to the fact that the aforementioned cluster formation may lead to a Volmer–Weber type three-dimensional growth mode. Sodium on $Cr_2O_3(0001)$, on the other hand, exhibits layer-by-layer growth [9].

At coverages around 3 ML the signal of metallic magnesium is found in the spectrum. Besides that, a small signal appears exactly at the expected position of the magnesium oxide signal, i.e. at 1180.7 eV. This provides clear evidence for the coexistence of magnesium metal and oxide at multilayer coverages.

As shown above, the deposition of magnesium on chromium oxide leads to a mixture of magnesium oxide, chromium oxide, magnesium metal and chromium metal on the sample surface already at 90 K. This result is comparable to previous findings in the system Na/NiO(111)/Ni(111) [8]. We also studied, as we did for Na/NiO, the temperature dependence of the chemistry in the system $Mg/Cr_2O_3(0001)/Cr(110)$ after deposition of approximately 7 ML magnesium at 90 K sample temperature. The Cr $2p_{3/2}$ spectra are shown as a function of temperature in Fig. 6. The left panel shows spectra taken at a near-normal detection angle whereas spectra in the right panel were taken at a grazing exit angle for the same preparation in order to enhance the surface sensitivity of the spectra.

The intensity at the low binding energy side of the main signal, indicative of the formation of chromium metal, is enhanced relative to the main line when the sample is heated. The intensity ratio between metal and the main oxide signal also increases for the grazing exit angle. These findings clearly prove the formation of chromium metal at elevated temperatures taking place on top of the chromium oxide film, i.e. near the Mg oxide interface.

We also performed experiments on the pure chromium oxide film at 1100 K, i.e. near the decomposition temperature of the oxide film, for two hours, in order to check for a possible diffusion of chromium metal through the oxide film or its formation on top in the absence of magnesium metal. The results are presented in Fig. 7. Spectra c and d, taken at 15° and 65° off-normal detection angle, exhibit only very little additional intensity indicating formation of chromium metal in comparison to spectrum a of the chromium metal Cr(110) surface, even though we are close to the decomposition temperature. Spectrum e shows the difference spectrum between c and d revealing no

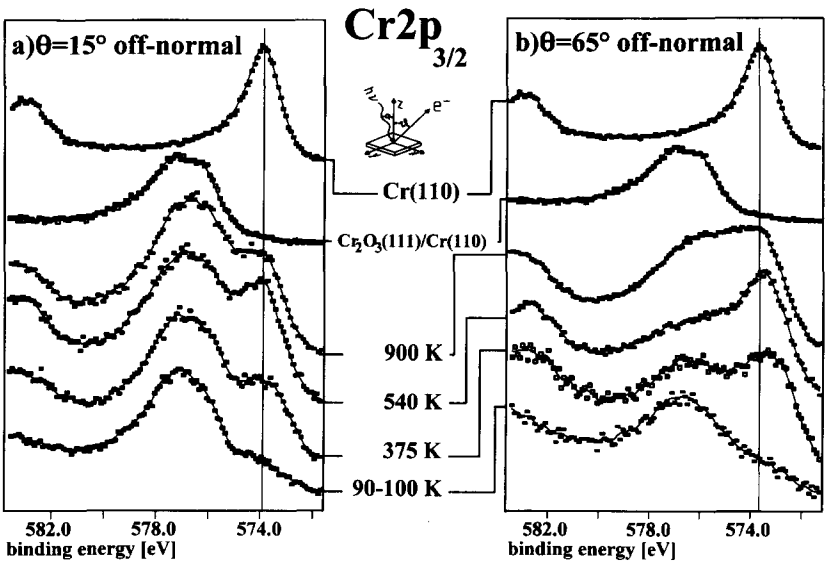

Fig. 6. Cr $2p_{3/2}$ XPS spectra after deposition of a thick Mg layer and subsequent heating obtained at near-normal (a) and grazing take-off angle (b) respectively in comparison to the spectra of clean chromium metal and chromium oxide film surfaces.

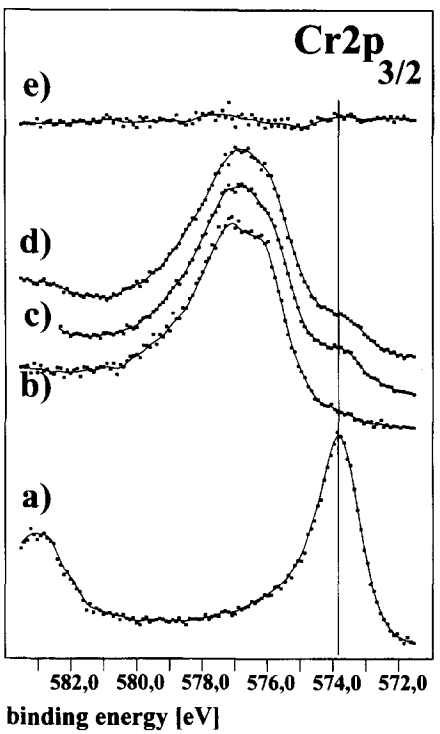

Fig. 7. Cr $2p_{3/2}$ XP spectra in a heating experiment of a chromium oxide thin film: (a) chromium metal Cr(110) surface; (b) chromium oxide surface freshly prepared; (c) after heating for 2 h at 1100 K, detection at 15° off-normal; (d) after heating for 2 h at 1100 K, detection at 65° off-normal; (e) difference spectrum of (c) and (d).

significant angular dependence of the additional intensity on the detection angle in contrast to the experiments involving magnesium metal (Fig. 6). In comparison to the heating experiment involving magnesium we conclude that heating the pure chromium oxide thin film at 1100 K (i.e. near decomposition temperature) leads to formation of very little chromium metal even at higher temperatures than in the presence of magnesium. A second difference between the two experiments is that in the former case the chromium metal is formed right at the surface of the oxide film whereas in the latter case the very small amount of metal seems to be distributed throughout the film. On the basis of these differences we can state that the temperature dependent reduction of the chromium oxide film is very strongly enhanced at the interface with a Mg metal deposit.

The magnesium 1s and 2p XPS spectra obtained after heating a magnesium metal deposit on chromium oxide are shown in Fig. 8a and b respectively. At 90 K the binding energies for metallic magnesium are identified at 1302.8 eV and 49.4 eV for the Mg 1s and the Mg 2p levels, respectively. They are shifted by about 1.5 eV and 1 eV towards higher binding energies, respectively, upon heating up to 900 K. According to the previous results, and in line with the literature [16], we deduce from our XPS data the formation of magnesium oxide.

An important difference between the Mg 1s and the Mg 2p spectrum is noticeable at 375 K. The Mg 1s spectral function shows additional intensity at the higher binding energy side but the spectrum is dominated by metallic magnesium. However, the situation becomes inverted in the Mg 2p spectrum where magnesium oxide contributes the major part to the spectral function at 375 K. This is due to different penetration depths of the photoelectrons. After excitation by Al Kα radiation (1486.6 eV) the kinetic energy of the Mg 1s photoelectrons is about 180 eV. In contrast to that, the kinetic energy of Mg 2p photoelectrons being excited by Mg Kα radiation (1253.6 eV) is about 1200 eV which means that the penetration depth is larger by about a factor of 10 than in the former case [17]. These

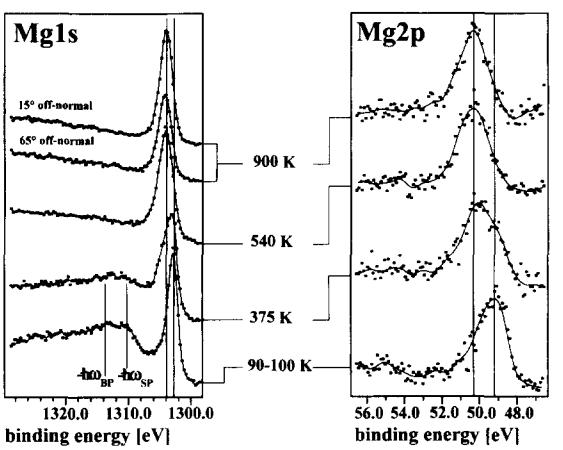

Fig. 8. Mg 1s (left panel) and 2p (right panel) XP spectra obtained after deposition of a thick Mg multilayer and subsequent heating. Bulk and surface plasmon losses are marked BP and SP respectively. If not indicated otherwise, the spectra were taken with 65° off-normal, i.e. grazing exit angle.

findings again lead to the conclusion that magnesium oxide is formed at the interface between magnesium metal and chromium oxide.

Photoelectron as well as Auger electron spectra of magnesium taken during the experiments exhibit extended loss structure on the lower kinetic energy side with respect to the main signal. In the present case these losses are due to plasmon excitations in metallic magnesium. In Fig. 5 the evolution of these loss features is observed during the deposition of magnesium at 90–100 K whereas Fig. 8 shows the disappearance of them upon heating a metallic magnesium film. This indicates the already mentioned transition of non-metallic to metallic magnesium in the former case and its reversal in the latter case.

Plasmon excitation spectra of small metal clusters are known to be influenced by their morphology [18] as well as by their electronic structure [19]. The plasmon frequency of metal clusters is red-shifted with decreasing size in comparison with the bulk plasmon frequency. Especially, the Mg Auger spectra taken during the deposition experiment (Fig. 5) exhibit an extended tailing to lower kinetic energies. This tailing could be indicative of clusters with statistically distributed size. With increasing coverage a magnesium multilayer is formed and the plasmon-loss structure evolves out of this tailing as can be observed between 3 ML and 7 ML coverage. A different evolution of plasmon loss features is found in the corresponding Mg 1s spectra (Fig. 5a). Here, the plasmon loss intensity starts to grow at a coverage of about 2.5 ML. Mg 1s photoelectrons were detected at a kinetic energy of 180 eV. This energy leads to high surface sensitivity of the spectra. On the other hand Mg $KL_{23}L_{23}$ spectra were taken at 1180 eV kinetic energy. In this case the electrons probe 10–15 Å of the sample [17]. We may conclude that the plasmon loss intensity in the Mg 1s spectrum of the 2.5 ML deposit is due to magnesium metal being located at the interface to the vacuum. Plasmonic losses in the Auger spectrum may be due to hidden metallic particles deeper inside the sample.

The Mg $KL_{23}L_{23}$ Auger spectra which are shown in Fig. 9 were obtained at detection angles of 15° and 65° off-normal for various temperatures.

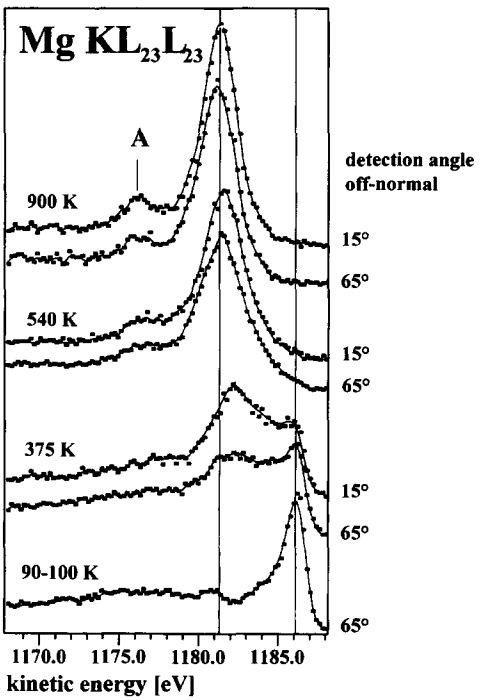

Fig. 9. Mg $KL_{23}L_{23}$-Auger spectra obtained after deposition of a thick Mg multilayer and subsequent heating. Feature A corresponds to the final state ^1S. The main signal is due to the ^1D final state. It is split by the octahedral crystal field into $^1T_{2g}$ and ^1E_g states. This causes the line width to exceed the resolution of the spectrometer as can be judged from a comparison to the spectrum of the metal film at 90 K.

As already discussed above, the spectrum at 90 K mainly represents magnesium metal accompanied by a weak signal indicating the presence of magnesium oxide even at this temperature. We stress that neither the Mg 1s nor the Mg 2p XP spectra allow for the identification of the small amount of MgO due to the smaller chemical shift in photoemission.

With increasing temperature the magnesium oxide signal is enhanced at the expense of the metal signal indicating the formation of magnesium oxide. We notice that the angular dependence at 375 K indicates the formation of magnesium oxide at the interface to the oxide film as discussed above. At 540 K the spectra are those of magnesium oxide with no angular dependence. Metallic magnesium is absent at this and higher temperature due to thermal desorption of magnesium multilayers. This can be judged from the heating experi-

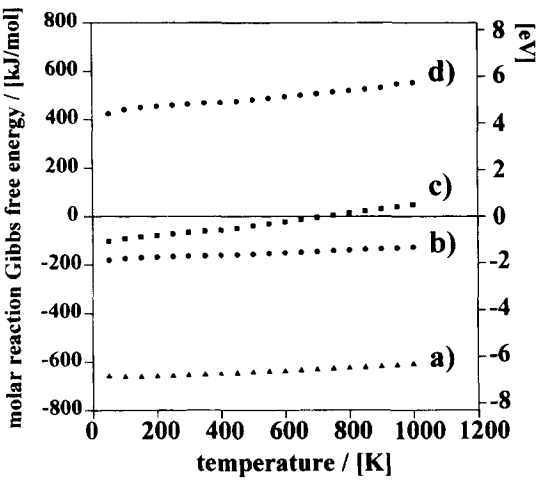

Fig. 10. Gibbs free energy for the oxygen exchange reactions: (a) $3Mg+Cr_2O_3 \rightarrow 3MgO+2Cr$; (b) $2Na+NiO \rightarrow Na_2O+Ni$; (c) $6Na+Cr_2O_3 \rightarrow 3Na_2O+2Cr$; (d) $6Na+Al_2O_3 \rightarrow 3Na_2O+2Al$. The values are taken for the bulk materials from Ref. [21].

ment on the system Mg/Cr(110) given in Fig. 2. Around 550 K the monolayer regime is reached. The corresponding LEED pattern is shown in Fig. 1e.

Hence, at 540 K the redox reaction can be considered complete due to the lack of Mg metal and consequently the Mg Auger spectra do not change towards higher temperature.

However, further changes can be observed in the intensity ratio of the Cr $2p_{3/2}$ spectra with regard to chromium oxide and metallic chromium in Fig. 6. The dominating features of metallic chromium in the spectra at 540 K are considerably decreased at 900 K. Since the reaction is already complete at this point we ascribe this to a redistribution of the products within the surface layer.

4. Conclusions and comparison with other systems

We have studied the surface chemistry of the system $Mg/Cr_2O_3(0001)/Cr(110)$ as a function of both coverage and temperature. At low temperatures the formation of chromium metal and magnesium oxide successively occurs as the coverage is increased. The reaction is limited to the interface between magnesium metal and chromium oxide due to kinetic hindrance of diffusion. This hindrance can be overcome at higher temperatures up to 540 K where magnesium multilayers desorb and the reaction stops.

In contrast to these results on magnesium, sodium, as discussed in detail elsewhere [9], does not lead to the formation of chromium metal on the chromium oxide film, regardless of temperature and coverage, although, on the basis of thermodynamic calculations of the bulk reaction, free energies indicate that this reaction is possible also for sodium [20]. On NiO(111), of course, sodium does induce the equivalent reaction. The bulk thermodynamic data are collected in Fig. 10. It is quite obvious that the reaction between Mg and Cr_2O_3 is exothermic for all considered temperatures by more than 6 eV. For sodium and NiO the free Gibbs reaction energy is exothermic by 1.5–2 eV only slightly varying with temperature. While Na cannot reduce Al_2O_3 at any considered temperature (endothermic by 4–6 eV) the Gibbs free energy changes between exothermicity and endothermicity for the system Na and chromium oxide near 700 K [20]. The energies involved in the latter case are of the order 0.5 to 1.0 eV. It is this energy range where it is very dangerous to deduce surface processes from the bulk thermodynamic data as the adsorption of sodium on chromium oxide indicates [9]. While this message is rather obvious it is much more difficult to pinpoint microscopically which processes are relevant. In fact, in the present paper the necessary data to discuss the individual steps, for example within the framework of a Born–Haber cycle, are not accessible and a final discussion must await these data. Theoretical calculations may help us in future to understand the initial steps in the interaction between an alkali metal atom and an oxide surface.

References

[1] H.-J. Freund, H. Kuhlenbeck and V. Staemmler, Rep. Prog. Phys. 59 (1996) 283.
[2] C. Lin, T. Ito, J. Wang and J.H. Lunsford, J. Am. Chem. Soc. 109 (1987) 4808.
[3] Physics and Chemistry of Alkali Metal Adsorption, Eds.

H.P. Bonzel, A.M. Bradshaw and G. Ertl, Material Science Monographs, Vol. 57 (Elsevier, Amsterdam, 1989).
[4] R.W. Gurney, Phys. Rev. 47 (1935) 479; J.W. Gadzuk, Surf. Sci. 6 (1967) 133; P. Nordlander and J.C. Tully, Phys. Rev. B 42 (1990) 5564.
[5] R.J. Behm, in: Physics and Chemistry of Alkali Metal Adsorption, Eds. H.P. Bonzel, A.M. Bradshaw and G. Ertl, Material Science Monographs, Vol. 57 (Elsevier, Amsterdam, 1989).
[6] R. Fasel, P. Aebi, J. Osterwalder and L. Schlapbach, Surf. Sci. 331–333 (1995) 80, and references therein.
[7] P.J. Hardman, R. Casanova, K. Prabhakaran, C.A. Muryn, P.L. Wincott and G. Thornton, Surf. Sci. 269–270 (1992) 677; R. Heise and R. Courths, Surf. Rev. Lett. 2 (1995) 147; Surf. Sci. 331–333 (1995) 1460; P.W. Murray, N.G. Condon and G. Thornton, Surf. Sci. 323 (1995) L281.
[8] M. Bender, K. Al-Shamery and H.-J. Freund, Langmuir 10 (1994) 3081.
[9] D. Ehrlich, M. Bender, I.N. Yakovkin, H. Kuhlenbeck and H.-J. Freund, to be published.
[10] M. Bender, D. Ehrlich, I.N. Yakovkin, F. Rohr, M. Bäumer, H. Kuhlenbeck, H.-J. Freund and V. Staemmler, J. Phys. Cond. Matt. 7 (1995) 5289.
[11] J.B. Benziger and R.J. Madix, J. Electron Spectrosc. Relat. Phenom. 20 (1980) 281.
[12] A. Stenborg and E. Bauer, Surf. Sci. 185 (1987) 394.
[13] H.W. King, in: Physical Metallurgy, Ed. R.W. Cahn (North-Holland, Amsterdam, 1970).
[14] A. Zangwill, Physics at Surfaces (Cambridge University Press, Cambridge, 1988).
[15] K.-H. Meiwes-Broer and H.O. Lutz, Phys. Blätter 47 (1991) 283.
[16] J.C. Fuggle, Surf. Sci. 69 (1977) 581.
[17] M.P. Seah, in: Practical Surface Analysis by XPS and AES, Eds. D. Briggs, M.P. Seah (Wiley, Chichester, 1983); M.P. Seah and W.A. Dench, Surf. Interf. Anal. 1 (1979) 2.
[18] W.A. de Heer, Rev. Mod. Phys. 65 (1993) 611.
[19] F. Reuse, S.N. Khanna, V. de Coulon and J. Buttet, Phys. Rev. B 41 (1990) 11743.
[20] L.F. Epstein and J. Nigriny, U.S. At. En. Com. Publ. AECD-3709 (1948).
[21] Handbook of Physics and Chemistry, 53rd ed. (CRC Press, Boca Raton, FL, 1972).